Separation and Purification Technology 81 (2011) 279–285

Contents lists available at ScienceDirect

Separation and Purification Technology

journal homepage: www.elsevier.com/locate/seppur

# Modeling of adsorption–reaction–desorption in granular media

Frank A. Coutelieris *

*Department of Environmental and Natural Resources Management, University of Ioannina, Seferi 2, GR-30100 Agrinio, Greece*

ARTICLE INFO

*Article history:*
Received 19 January 2011
Received in revised form 18 July 2011
Accepted 19 July 2011
Available online 4 August 2011

This work is dedicated to the memory of my supervisor Prof. Alkiviades Ch. Payatakes.

*Keywords:*
Convection
Diffusion
Adsorption
Mass transfer
Flow
Granular media

ABSTRACT

The scope of this work is to model the mass transport process from a moving Newtonian fluid to an assemblage of spherical solid absorbers. The flow field for laminar flow was obtained by numerically solving the Navier–Stokes equation in the pore space of a stochastically constructed three-dimensional assemblage of spherical particles, where the convective/diffusive transport is simulated by involving an adsorption/reaction/desorption mechanism as an appropriate boundary condition. The spatial/volume-averaging technique was used here for up-scaling, where the simplified boundary-value problems have been described and numerically solved for the velocity field and concentration. Macroscopic mass transfer coefficient was then calculated and compared with other approaches. The process was found to be controlled by the Peclet number as well as the porosity of the porous structure. Through model validation, the sorption mechanism considered here proved to provide a reasonable estimation of the mass transfer.


## 1. Introduction

There are many industrial and technological applications regarding mass transport within porous media in a variety of scientific fields, such as environment, energy and biology [1–3]. Mathematical modeling of transport processes in porous media is a powerful tool, especially when experimental observations are difficult, time consuming, or expensive. The complexity of the mathematical description of mass transport in realistic porous structures is significantly high, due to the coupling between the physicochemical mechanisms and the local geometry of the porous medium. Modeling becomes more difficult when moving from the pore level to the field level, because different length scales result in complicated descriptions of the problem's physics and therefore increased computational power is usually required.

From the late 1950s, special effort has been given to mathematically describe and solve flow and mass transport problems in porous media, initially for quite simplified geometries where analytical solutions can be obtained for the flow field and mass diffusion and/or adsorption process [4–9]. On the other hand, numerical solutions in realistic reconstructions of porous media for the Stokes equations and the relative transport problems have been obtained for several specific applications during the last decades [10–14]. For the majority of the above research, the particles were assumed to adsorb mass instantaneously, which is obviously a rare physicochemical phenomenon. Only recently, some more detailed models for the sorption mechanism have been presented [15,16].

An extended version of the above-mentioned approach is adopted here to simulate the adsorption–heterogeneous reaction–desorption mechanism, which can accurately describe the sorption upon a solid surface of a solute diluted in the flowing fluid [17,18]. More specifically, it can be considered that the solute diluted in the bulk phase is initially adsorbed by the solid surface where a heterogeneous reaction takes place and its products, which are assumed to be inactive and of very low concentrations, are again desorbed in the bulk phase. The adsorption is assumed to occur due to vacant sites that are normally distributed over the surface area while the whole process is determined by an overall rate according to the flow regime and thermodynamics [19].

The major issue of typical macroscopic modeling for such cases (or even simpler) can be identified at the *a priori* definition of some macroscopic quantities necessary to solve equations, although normally derived from the solution of these equations. So far, mainly empirical or semi-empirical correlations for these parameters have been proposed based on experimental measurements of specific systems [20,21]. On the other hand, the generalized treatment of such a problem corresponds to theoretical estimations of these quantities where the volume averaging concept is a frequently employed tool for the large scale modeling of processes taking place in porous media, eliminating the influence of porous geometry on transport results [22–24]. Starting from transport

* Tel.: +30 26410 74196; fax: +30 26410 39576.
*E-mail address:* fkoutel@cc.uoi.gr

1383-5866/$ - see front matter © 2011 Elsevier B.V. All rights reserved.
doi:10.1016/j.seppur.2011.07.028

**Nomenclature**

| | |
|---|---|
| $A_{LS}$ | area of the liquid-solid interface |
| $C_L$ | concentration of the tracer in the liquid phase |
| $C_{LS}$ | concentration of the tracer on the solid surface |
| $D_L$ | molecular diffusivity of diffusing species in the liquid phase |
| $k_a$, $k_d$, $k_s$ | adsorption, desorption and heterogeneous reaction rate constants, respectively |
| $L$ | characteristic length of liquid phase |
| $N$ | Avogadro's number |
| $n$ | order of the heterogeneous reaction |
| $\mathbf{n}_{LS}$ | unit normal vector directed from liquid to solid phase |
| $p$ | pressure field of flowing liquid phase |
| $Pe$ | Peclet number defined in the liquid phase [$=\langle\mathbf{v}\rangle^L L/D_L$] |
| $R_n$ | rate of sorption occurring on the liquid–solid interface |
| $r_n$ | dimensionless sorption rate |
| $u$ | dimensionless velocity field in the β-phase |
| $\mathbf{v}$ | velocity field in the β-phase |
| $V$ | total volume |
| $V_L$ | volume of liquid phase |
| $y$ | dummy quantity associated with β-phase |

*Greek letters*

| | |
|---|---|
| $a^*$ | dimensionless mass transfer coefficient |
| $\varepsilon_L$ | volume fraction of the liquid phase |
| $\zeta_L$ | transformed variable, used in Eq. (5) |
| $\mu$ | viscosity of flowing liquid phase |
| $\xi_m$ | total number of available sites for sorption |
| $\phi_L$ | scalar variable used for the decomposition, as in [21,26] |

*Other symbols*

| | |
|---|---|
| $\langle Q\rangle$ | superficial volume average of any quantity $Q$ |
| $\langle Q\rangle^L$ | interstitial volume average of any quantity $Q$ in the liquid phase |

equations at the micro-scale (pore) level, the spatial averaging theorem is applied along with the proper assumptions, leading to the estimation of macroscopic quantities such as mass transfer coefficient and dispersion tensor [25]. To further simplify the mathematical modeling and eliminate the simulation effort, the majority of the above-mentioned models have been applied in quite simplistic domains, such as unit cells, since the focus was on the interfacial mass exchange rather than the representation of the medium in a realistic manner.

All the above concepts have been applied to granular media by Coutelieris et al. [16] where the mass transport problem was solved when an adsorption/reaction/desorption mechanism described adsorption of the diluted mass on the solid adsorbers (particle) surface. A comparison of different sorption mechanisms in terms of adsorption efficiency was also included in this research, where the assumption of instantaneous adsorption was found to greatly overestimate adsorption efficiency compared to that obtained using the adsorption–reaction–desorption model. The particle-in-cell concept has been adopted here. The idea behind this concept is the "cell approach", where the medium is considered an assemblage of unit cells gathered in a regular manner. Accordingly, it was widely accepted that the unit cell adequately represents the entire medium, therefore processes occurring through the porous structure are described sufficiently by those occurring in the unit cell. As grains are usually spherical, sphere-in-cell models are based on the representation of the overall solid mass of the swarm by a solid spherical body embedded in a spherical liquid envelope. The boundary conditions imposed on the outer surface of the envelope are supposed to adequately represent the interactions with other grains of the swarm. Obviously, the thickness of the surrounding fluid layer is adjusted so the ratio of the solid volume to the volume of the liquid envelope represents exactly the solid volume fraction of the porous medium. The main advantage of these models is that an analytical expression for the stream function can be obtained much easier than in numerical investigations. The spherical shape corresponds to a formulation that leads to axially symmetric flow and that has a simple analytical solution of closed form which can therefore be readily used for heat and mass transport calculations.

In the present work, the adsorption/heterogeneous reaction/desorption mechanism applied in [16] was applied for the convection-diffusion problem in stochastically constructed three-dimensional sphere assemblages, which are assumed to represent granular porous media. The aim is to apply the spatial averaging approach to these complicated processes to quantify mass transfer from fluid to solid phases of the medium and to investigate how different geometrical and physicochemical parameters (i.e. porosity, diffusivity and Peclet number) affect it. To demonstrate the validity of this approach, the present model has been verified against other simulation and experimental results.

## 2. Mathematical formulation

The area of interest is a porous domain consisting of a flowing aqueous phase ($L$-phase) and a solid phase ($S$-phase). A tracer is advected by the flowing liquid phase, being sorpted in the liquid–solid interface. The governing processes are diffusion and advection in the liquid phase while the liquid–solid interface is characterized by the adsorption/reaction/desorption mechanism of the tracer (see below).

By assuming that the bulk phase is chemically neutral, the pore-level transport of the tracer in the β-phase is described by the steady state convection-diffusion equation:

$$\nabla\cdot(\mathbf{v}C_L) = D_L\nabla^2 C_L \tag{1}$$

where $C_L$ is concentration, $\mathbf{v}$ is the fluid velocity and $D_L$ is the diffusivity in the liquid phase.

To assure the continuity of the mass fluxes on the solid–liquid interfaces, the following boundary condition is applied:

$$\mathbf{n}_{LS}\cdot\nabla C_L = R_n \quad \text{at} \quad A_{LS} \tag{2}$$

where the overall sorption rate $R_n$ is dependent on the type of sorption process considered. For a typical adsorption/heterogeneous reaction/desorption mechanism for the tracer upon the solid surface [18,19], the rate $R_n$ is given as:

$$R_n = k_s C_{LS}^n \tag{3}$$

where $k_s$ is the rate constant of the heterogeneous reaction of order $n$ upon the surface. By considering a three step (adsorption/heterogeneous reaction/desorption) concept of the sorption process involving the theory of active (vacant) sites [18,15,16], and by assuming very rapid (instantaneous) desorption for the chemically neutral desorbed product, the equality of the rates per step corresponds to a non-linear equation for the concentration of the tracer upon the solid surface, $C_{LS}$, as follows [15]:

$$k_s C_{LS}^n + [k_d + k_a C_L N]C_{LS} - k_a C_L \xi_m = 0 \tag{4}$$

where $k_a$ and $k_d$ denote the adsorption and desorption rate constants of the tracer, respectively, $\zeta_m$ is the total number of available sites for sorption and $N$ is the Avogadro's number. The first term of the above equation represents the molar flux due to the reaction, the second term corresponds to the mass flux approaching the surface, and the final term describes the flux due to adsorption [16]. Overall, the above equation correlates the hard-to-measure surface concentration of the tracer, $C_{LS}$, with the concentration in the bulk phase very close to the solid surface, $C_L$, by considering the balance for the active sites on the adsorbing surface. In general, only the cases of $n = 0$, $n = 1$ and $n = 2$ are of practical importance but zero order reactions have very limited applications [18]. Therefore, the present investigation deals only with first ($n = 1$) and second ($n = 2$) order heterogeneous reactions. Finally, it should be stressed that this boundary condition implies non-linearity in the whole approach.

As shown elsewhere [21,22,25], the solution of the micro-scale mass transport problem and the analogous micro-scale flow-field is not sufficient to accurately represent macroscopic quantities such as mass transport coefficient. To solve this, the volume-averaging technique has been found a powerful tool [21–26]. Following this procedure, which is presented briefly in Table 1 and in detail elsewhere [21,26], the above problem can be transformed to the following dimensionless system:

$$Pe\mathbf{u} \cdot \nabla\zeta_L = \nabla^2\zeta_L - \varepsilon_L^{-1} \quad \text{in the liquid phase} \tag{5}$$

$$\mathbf{n}_{LS} \cdot \nabla\zeta_L = r_n \quad \text{at} \quad A_{LS} \tag{6}$$

where $Pe = \frac{\langle \mathbf{u} \rangle^L L}{D_L}$ is the Peclet number defined in the liquid phase by using a length $L$ characteristic for this phase, $\mathbf{u}$ is the dimensionless velocity vector, $\zeta_L$ is the scalar variable used for the decomposition, and $r_n$ is the dimensionless sorption rate.

The dimensionless mass transfer coefficient is simply [21,26]:

$$\alpha^* = -\frac{\varepsilon_L}{\langle \zeta_L \rangle} \tag{7}$$

Brackets denote averages over the total volume $V$ or the volume of the aqueous phase, $V_L$, where the superficial volume average is defined as:

$$\langle y_L \rangle = \frac{1}{V} \int_{V_L} y_L dV \tag{8a}$$

and the interstitial volume average as:

$$\langle y_L \rangle^L = \frac{1}{V_L} \int_{V_L} y_L dV \tag{8b}$$

**Table 1**
The spatial averaging technique (as in [21,26]).

| | Differential equations with boundary and compatibility conditions | Mass transfer coefficient |
|---|---|---|
| Pore level formulation | $\nabla \cdot (\mathbf{v}C_L) = D_L \nabla^2 C_L$<br>$\mathbf{n}_{LS} \cdot \nabla C_L = R_n$ at $A_{LS}$ | |
| Decomposition<br>$C_L = \langle C_L \rangle^L + C'_L$<br>$\mathbf{v}_L = \langle \mathbf{v}_L \rangle^L + \mathbf{v}'_L$ | $\mathbf{v} \cdot \nabla s_L = D_L \nabla^2 s_L - \varepsilon_L^{-1} \alpha$ | $\alpha = \frac{D_L}{V} \int_{A_{LS}} \mathbf{n}_{LS} \cdot \nabla s_L dA$ |
| | $\mathbf{n}_{LS} \cdot \nabla s_L = R_n$ at $A_{LS}$<br>$\langle s_L \rangle = 0$ | |
| Transformation $s_L = 1 + \alpha^* \zeta_L$ | $Pe\mathbf{u} \cdot \nabla\zeta_L = \nabla^2\zeta_L - \varepsilon_L^{-1}$<br>$\mathbf{n}_{LS} \cdot \nabla\zeta_L = R_n$ at $A_{LS}$ | $\alpha^* = -\frac{\varepsilon_L}{\langle \zeta_L \rangle}$ |

## 3. Simulations

### 3.1. Geometry

To define a 3D domain to solve flow and transport problems, a granular porous medium was constructed in the form of a spherical particle assemblage. Specifically, representation of the domains under consideration was achieved as follows:

Step 1. Define values for (a) porosity and (b) active surface area.
Step 2. Calculate the mean grain diameter by assuming uniform grain distribution.
Step 3. By using a random number generator, select the position of the sphere's center, being in a box of specified dimensions ($3 \times 2 \times 3$ mm, see [32]).
Step 4. By using a random number generator, select a radius supposed to follow the log-normal distribution.
Step 5. Check if the void space around the sphere is free: if "yes", accept the radius value, otherwise repeat Step 4 above.
Step 6. Pose the sphere.
Step 7. Repeat Steps 3–6 until the volume of the positioned spheres satisfies the pre-defined porosity value.
Step 8. Calculate the mean diameter of the grains.
Step 9. Compare with the pre-defined mean diameter.
Step 10. Repeat Steps 3–9 until the relative difference between the pre-defined mean diameter and the calculated mean diameter is lower than 0.001%.

The surface to volume ratio, S/V, for a typical porous medium of porosity 0.43 is approximately 10,000 [27]. This corresponds to a mean grain diameter of ~0.00056 m and ~110 spheres. These values may vary slightly due to statistics (log-normal distribution for sphere diameters) but this variation should be kept below 2% to satisfy the convergence criteria in Steps 7 and 10 of the above algorithm. A graphical representation of the abovementioned representative medium is presented in Fig. 1 and a randomly selected 2D cut of this domain in is shown Fig. 2, where the grid for the numerical solution is also depicted (see below). Obviously, many three-dimensional realizations could be generated by the above algorithm for a specific porosity value. Therefore, it is necessary

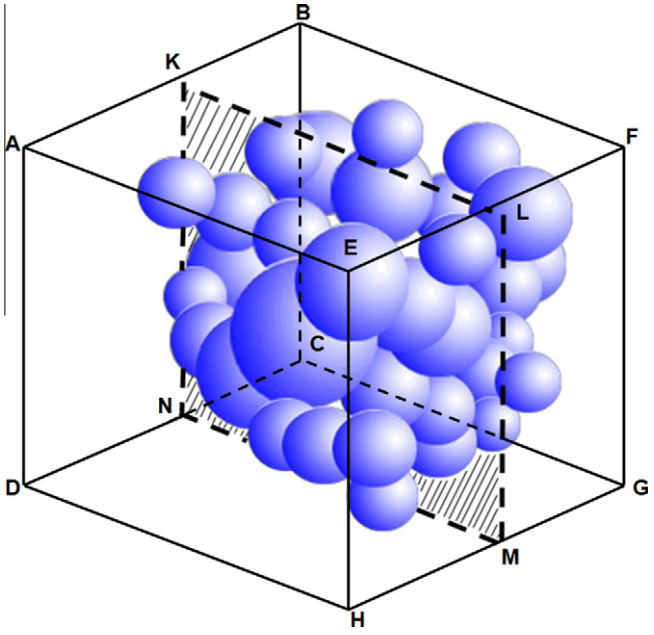


**Fig. 1.** A three-dimensional representation of the porous medium.

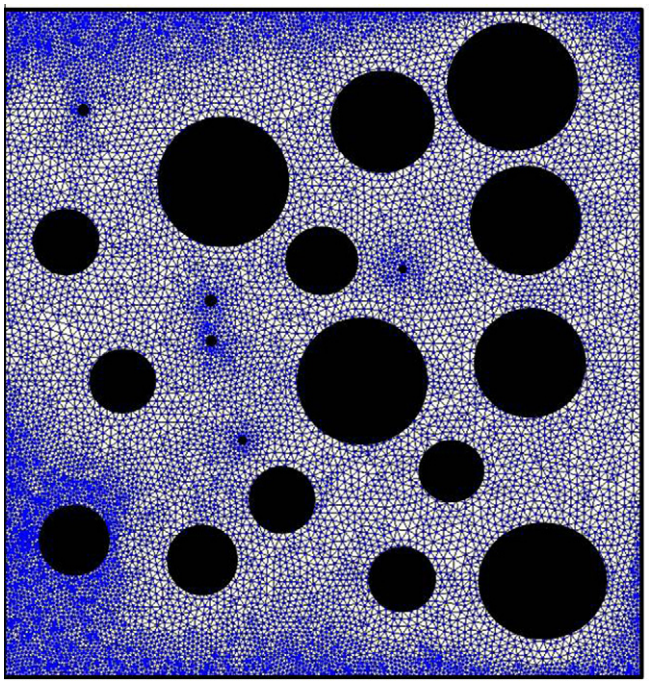

**Fig. 2.** A selected two-dimensional cut of the simulated geometry discretized by an unstructured grid.

to validate the results against these configurations to ensure that the macroscopic results are independent of each specific realization. Such a validation will follow.

### 3.2. Algorithm

To adequately simulate the above-described problem, an algorithmic procedure was developed as follows:

- Solve the flow problem at the microscopic level and calculate interstitial and superficial velocity fields.
- Formulate the mass transport problem at the microscopic level.
- Decompose local velocity and concentration in terms of an interstitial average and a fluctuation.
- Describe concentration fluctuations in terms of linear combinations of interstitial averaged concentration and its gradient.
- Solve the closure problem.
- Integrate the resulting quantities to calculate macroscopic coefficients.

### 3.3. Numerical scheme

The size of the digitized domains was $102 \times 102 \times 102$ grid points for all the simulations, corresponding to an unstructured grid consisting of more than 1 million cells (see Figs. 1 and 2). The grid spacing was chosen to be non-uniform because it has been proved that appropriately non-uniform discretization performs better than the equal-spaced one [28]. For the numerical solution of the closure boundary value problem, a non-uniform finite difference scheme with upwinding was used and the resulting linear systems of equations were solved using Successive Over-Relaxation (SOR), which is accurate enough for such a system. Finally, a numerical algorithm involving a typical Newton method for non-linear systems in conjunction with the finite differences scheme, was modified and adopted to handle the non-linearity of the system, when necessary [29]. This is because the heterogeneous reactions of orders higher than one introduce nonlinearity into the system through the boundary condition described by Eq. (3). To achieve convergence at each time step, the values of the residuals for all the unknown quantities (velocity components, concentration) should be lower than $10^{-4}$. For those purposes, the numerical solution for the problem described above was obtained using a FORTRAN code and the computational needs were satisfied by an Intel Pentium 3.2 GHz computer. The steady-state condition was assumed to be achieved whenever the relative difference for all the results of two sequential time-steps was lower than 0.001%. Given a specific randomly constructed domain, the necessary time for each run was approximately 12 hours (including the solution for the flow-field).

### 3.4. Boundary conditions

Further to the inner boundary condition for mass exchange on the solid–liquid interface (described by Eq. (3)), the outer boundary conditions are: constant concentration has been applied at the inlet (face ABCD at Fig. 1), zero concentration has been applied at the outlet (face EFGH at Fig. 1), and periodicity has been applied at to the other four surfaces (ABEF with DHGC and AEDH with BFGC in Fig. 1).

### 3.5. Flow-field

The velocity field was computed numerically by solving the Stokes equations

$$\nabla p = \mu \nabla^2 \mathbf{v} \tag{9a}$$

$$\nabla \cdot \mathbf{v} = 0 \tag{9b}$$

$$\mathbf{v} = \mathbf{0} at A_{\beta\sigma} \tag{9c}$$

where $\mathbf{v}$, $p$, and $\mu$ are the velocity vector, pressure and fluid viscosity, respectively. Regarding outer boundary conditions, constant pressure drop has been applied between inlet and outlet (faces ABCD and EFGH at Fig. 1), while periodical conditions have been applied to the other surfaces. The velocity $\mathbf{v}$ at any point has been afterwards normalized with the characteristic velocity magnitude

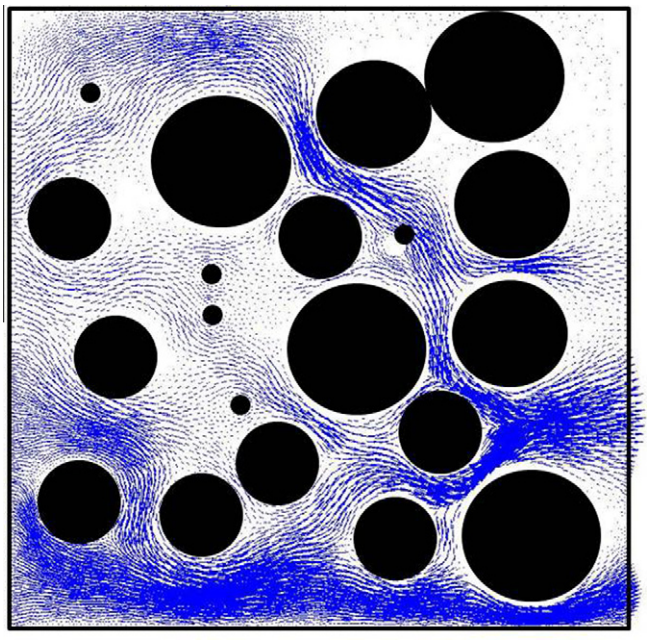

**Fig. 3.** Flow field in the representative porous medium.

to obtain the dimensionless velocity **u** used in Eq. (5). The procedure for solving the 3D Stokes flow problem involves discretization in terms of three-dimensional elements and was as follows [30]: At the pore level, a staggered marker-and-cell (MAC) mesh [30,31] is used, with the pressure defined at the center of the cell and the velocity components defined along the corresponding face boundaries. The resulting linear system of equations is solved by a successive over-relaxation (SOR) method. An initial guess for $p$ is determined through the solution of a Laplace equation. Next, the velocity vector **v** is calculated from the corresponding momentum balance and the continuity equation $\nabla \cdot \mathbf{v} = 0$. The pressure is corrected through an artificial compressibility equation of the form [30–32]:

$$\frac{dp}{dt} = \nabla \cdot \mathbf{v} \tag{10}$$

This approach to determine the velocity field has been widely validated elsewhere in terms of both the velocity field and corresponding permeability [31]. A typical result for the above-mentioned flow-field is depicted in Fig. 3, where a 2D cut of the medium (the same as in Fig. 2) is considered in order for the velocity vector to be visualized clearly.

## 4. Results and discussion

The results were initially validated against the randomness of the structure, as previously discussed. More precisely, the mass transfer coefficient $a^*$ was calculated for several different depositions of spheres while the porosity value was kept constant (=0.43). It was found that the random deposition does not significantly affect mass transfer to the solid phase, as shown in Table 2. Dependence of the solution on the grid was then also examined in terms of mass transfer coefficient. It was found that a discretization of $102 \times 102 \times 102$ points is more than sufficient for adequate calculations (see Table 3). It must be noted that the parametric analysis for the grid influence is limited in the order only, as this is the parameter that introduces the non-linearity, thus the solution and the grid are more sensitive in it.

The relative agreement between the results produced by considering the approximation by [16] and those obtained using the above technique is presented in Fig. 4. By assuming a typical value for $\xi_m$ (1 active site per Å$^2$), the values of the sorption constants were (before the non-dimensionalization of the problems) $k_a = 1 \times 10^{-30}$ m$^3$ s$^{-1}$, $k_d = 8 \times 10^{-3}$ s$^{-1}$ and $k_s = 8 \times 10^{-3} \times 100^{(1-n)}$ (kg m$^{-2}$)$^{1-n}$ $s^{-1}$. These values can be considered as typical [18] and are used in the simulations presented here unless otherwise stated. The figure compares the respective mass transfer coefficient for the standard porosity $\varepsilon = 0.43$ while the adsorption/reaction/desorption mechanism includes heterogeneous reaction of first ($n = 1$) and second ($n = 2$) order. Regarding the pore-level simulations from [16], a discrepancy from the results of the current model is always observed, thus indicating the underestimation of macroscopic mass transport quantities when calculated using pore-level

**Table 2**
Independence on the random deposition ($\varepsilon_L = 0.43$).

| Different random assemblages | *Pe* | *n* | $a^*$ |
|---|---|---|---|
| Case 1 | 1 | 1 | 20.93 |
| Case 2 | 1 | 1 | 20.83 |
| Case 3 | 1 | 1 | 21.01 |
| Case 4 | 1 | 1 | 20.77 |
| Case 5 | 1 | 1 | 20.96 |
| Case 1 | 100 | 1 | 46.55 |
| Case 2 | 100 | 1 | 45.87 |
| Case 3 | 100 | 1 | 46.11 |
| Case 4 | 100 | 1 | 47.02 |
| Case 5 | 100 | 1 | 46.39 |
| Case 1 | 1 | 2 | 19.36 |
| Case 2 | 1 | 2 | 19.91 |
| Case 3 | 1 | 2 | 19.07 |
| Case 4 | 1 | 2 | 18.66 |
| Case 5 | 1 | 2 | 19.12 |
| Case 1 | 100 | 2 | 45.88 |
| Case 2 | 100 | 2 | 45.01 |
| Case 3 | 100 | 2 | 46.99 |
| Case 4 | 100 | 2 | 45.85 |
| Case 5 | 100 | 2 | 46.02 |

**Table 3**
Grid independence ($\varepsilon_L = 0.43$, $Pe = 1$).

| Grid points | *n* | $a^*$ |
|---|---|---|
| 10648 | 1 | 19.46 |
| 74088 | 1 | 22.23 |
| 238328 | 1 | 16.44 |
| 551368 | 1 | 19.02 |
| 1061208 | 1 | 20.93 |
| 3511808 | 1 | 20.93 |
| 10648 | 2 | 11.34 |
| 74088 | 2 | 9.81 |
| 238328 | 2 | 12.67 |
| 551368 | 2 | 15.40 |
| 1061208 | 2 | 19.36 |
| 3511808 | 2 | 19.36 |

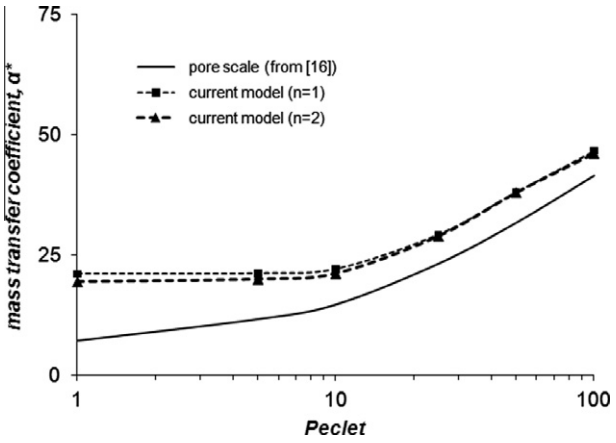


**Fig. 4.** Comparison between the results of the current model with those found in the literature.

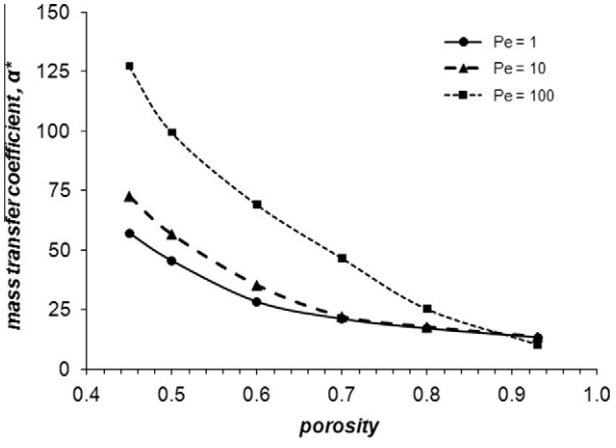


**Fig. 5.** The influence of porosity on mass transport.

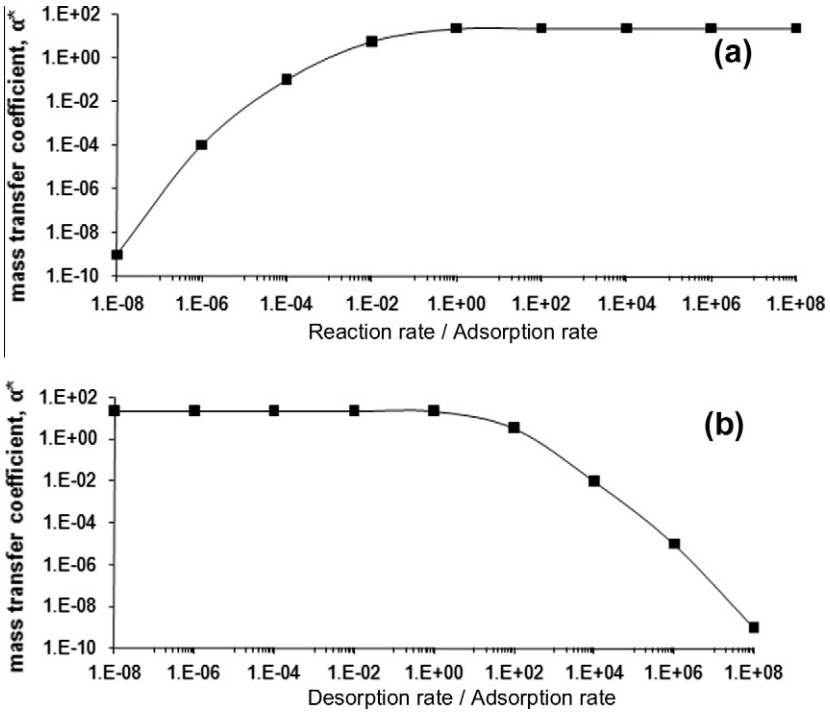


**Fig. 6.** Dependence of mass transport on the ratio of the reaction to the adsorption rates (a) and on the ratio of desorption to adsorption rates (b).

approaches in small-scale domains, as mentioned in related literature [33]. In terms of physical interpretation, Fig. 4 depicts the effect of convection on mass transport, where it is shown that the stronger the convection, the more efficient the tracer transport from the fluid to the solid phase, at least for low and intermediate porosity values, which correspond to relatively high amounts of solid absorbers in the medium that are active and absorb the tracer. Finally, the order of the reaction does not seem to significantly affect the results, or the agreement between the two approaches. Only first order reaction is considered hereafter.

The influence of the volume porosity of the medium on mass transport is presented in Fig. 5. It is clearly shown that porosity is an unfavorable parameter for adsorption, since the void space increases as porosity increases (although the active solid surface area does not necessarily decrease), thus corresponding to high possibility for the tracer to escape from the porous material through the void space. For high porosity values, as Peclet values increase, the transport process becomes more and more convective, thus the mass transport becomes less effective, i.e. high amounts of the tracer have the ability to escape from the medium. On the other hand, low porosity values correspond to large amounts of solid phase in the medium, thus convection favors mass transport since the tracer is forced to approach the absorbing surfaces. These two competitive phenomena are translated through the cross of the curves shown in Fig. 5, which correspond to a porosity value where both mechanisms are of equivalent strength. This value obviously depends on the specific flow and transport characteristics.

Fig. 6 depicts the relative influence of the sorption mechanism, i.e. the reaction, adsorption and desorption rates, on the mass transport. More precisely, Fig. 6a presents the mass transfer coefficient as a function of the ratio of tracer destruction rate due to the reaction, divided by the tracer destruction rate due to adsorption. In any case, the values of the rate constants not involved in these ratios were kept standard. It is observed that the decrement of the reaction rate (for constant adsorption rate) corresponds to a consequent decrement of the mass transport because the tracer has been adsorbed but not destroyed at the same rate and, therefore remains on the surface filling the vacant sites, i.e. setting barriers in the sorption process of the tracer. On the other hand, the increment of reaction rate forces the adsorption to tend asymptotically to a constant value which depends on the geometrical characteristics of the medium. Fig. 6b shows the influence of the ratio desorption/adsorption rate on the mass transport for heterogeneous reaction of the first order. It is observed that the increment of the desorption rate beyond a critical value corresponds to a decrease of this transport to very low values. It is important to note that the value attained by the mass transfer coefficient before the critical desorption rate is the same as the asymptotic value of Fig. 6a, further underlying its independence from the reaction characteristics.

## 5. Conclusions

In this paper, the mass transport from a moving Newtonian fluid to an assemblage of spherical solid absorbers is presented and the effective mass transfer coefficient between the fluid and the solid phases is derived. By using the volume-averaging method, the relative closure problem has been defined and applied in a three-dimensional artificial representation of a typical granular porous medium. In addition, a numerical solution of the flow-field and the corresponding convection-diffusion problem has been achieved in stochastically constructed three-dimensional sphere assemblages. In all cases, a sorption mechanism involving first and second order heterogeneous reaction has been considered. The numerical solution within this domain allows for the calculation of the effective mass transfer coefficient. The problem was shown to be controlled by the Peclet number, while it was found that higher mass transport corresponds to lower porosity and increasing Peclet numbers lead to higher mass transport when the porosity remains low enough to ensure adequate solid mass within the medium.

## Acknowledgments

The author would like to thank Dr. A. Stubos and Dr. M. Kainourgiakis from the National Centre for Scientific Research "Demokritos", Greece, for their useful discussions on the topic, as well as Dr. Eleni Vakouftsi from the University of Western Macedonia, Greece, for her technical assistance.

## References

[1] P. Meakin, A.T. Skjeltorp, Application of experimental and numerical models to the physics of multiparticle systems, Adv. Phys. 42 (1993) 1–127.
[2] T.G. Ellis, E. Eliosov, C.G. Schmit, K. Jahan, K.Y. Park, Activated sludge and other aerobic suspended culture processes, Water Environ. Res. 74 (2002) 385–410.
[3] F.J. Valdes-Parada, J.A. Ochoa-Tapia, J. Alvarez-Ramirez, Effective medium equations for fractional Fick's law in porous media, Phys. A. 373 (2007) 339–353.
[4] J. Happel, Viscous flow in multiparticle systems: slow motion of fluids relative to beds of spherical particles, AIChE J. 4 (1958) 197–201.
[5] S. Kuwabara, The forces experienced by randomly distributed parallel circular cylinders or spheres in a viscous flow at small Reynolds numbers, J. Phys. Soc. Jpn. 14 (1959) 527–532.
[6] V.G. Levich, Physicochemical Hydrodynamics, Prentice-Hall, New Jersey, 1962.
[7] R. Pfeffer, Heat and mass transport in multiparticle systems, Ind. Eng. Chem. Fund. 3 (1964) 380–383.
[8] G.H. Neale, W.K. Nader, Prediction of transport processes within porous media – diffusive flow processes within an homogeneous swarm of spherical particles, AIChE J. 19 (1973) 112–119.
[9] F.A. Coutelieris, V.N. Burganos, A.C. Payatakes, On mass transfer from a Newtonian fluid to a swarm of adsorbing spheroidal particles for high Peclet numbers, J. Colloid Interf. Sci. 161 (1993) 43–52.
[10] G.I. Tardos, C. Gutfinger, N. Abuaf, High Peclet mass transfer to a sphere in a fixed or fluidized bed, AIChE J. 22 (1976) 1147–1150.
[11] V.V. Mourzenko, S. Bekri, J.F. Thovert, P.M. Adler, Deposition in fractures, Chem. Eng. Com. 150 (1996) 431–464.
[12] S. Bekri, J.F. Thovert, P.M. Adler, Dissolution and deposition in fractures, Eng. Geol. 48 (1997) 283–308.
[13] A. Ahmadi, A. Aigueperse, M. Quintard, Calculation of the effective properties describing active dispersion in porous media: from simple to complex porous media, Adv. Water Res. 24 (2001) 423–438.
[14] G.E. Kapellos, T.S. Alexiou, A.C. Payatakes, A multiscale theoretical model for diffusive mass transfer in cellular biological media, Math. Biosci. 210 (2007) 177–237.
[15] F.A. Coutelieris, V.N. Burganos, A.C. Payatakes, Model of adsorption–reaction–desorption in a swarm of spheroidal particles, AIChE J. 50 (2004) 779–785.
[16] F.A. Coutelieris, M.E. Kainourgiakis, A.K. Stubos, Low to moderate Peclet mass transport in assemblages of spherical particles for a realistic adsorption–reaction–desorption mechanism, Powder Tech. 159 (2005) 173–179.
[17] M.H. Peters, R.K. Jalan, D. Gupta, A dynamic simulation of particle deposition on spherical collectors, Chem. Eng. Sci. 40 (1985) 723–731.
[18] P. Atkins, J. De Paula, Physical Chemistry 7th ed., Freeman, New York, 2001.
[19] J.M. Smith, Chemical Engineering Kinetics, McGraw-Hill, Tokyo, 1981.
[20] V.N. Burganos, F.A. Coutelieris, A.C. Payatakes, Sherwood number for a swarm of adsorbing spheroidal particles at any Peclet number, AIChE J. 43 (1997) 844–846.
[21] M. Quintard, S. Whitaker, Convection dispersion and interfacial transport of contaminants, Adv. Water Res. 17 (1994) 221–239.
[22] S. Whitaker, Diffusion and dispersion in porous media, AIChE J. 13 (1967) 420–427.
[23] F. Zanotti, R.G. Carbonell, Development of transport equations for multiphase systems I: general development for two-phase systems, Chem. Eng. Sci. 39 (1984) 263–278.
[24] F. Zanotti, R.G. Carbonell, Development of transport equations for multiphase systems II: application to one-dimensional axi-symmetric flows of two-phases, Chem. Eng. Sci. 39 (1984) 279–297.
[25] M. Quintard, S. Whitaker, Transport in ordered and disordered porous media: volume averaged equations, closure problems and comparison with experiments, Chem. Eng. Sci. 48 (1993) 2537–2564.
[26] F.A. Coutelieris, M.E. Kainourgiakis, A.K. Stubos, E.S. Kikkinides, Y.C. Yortsos, Multiphase mass transport with partitioning and inter-phase transport in porous media, Chem. Eng. Sci. 61 (2006) 4650–4661.
[27] J.S. Newman, C.W. Tabias, Theoretical analysis of current distribution in porous electrodes, J. Electrochem. Soc. 109 (1962) 11831191.
[28] L.M. Sun, P. LeQuere, M.D. Levan, Numerical simulation of diffusion-limited PSA process models by finite difference methods, Chem. Eng. Sci. 51 (1996) 5341–5352.
[29] R.L. Burden, J.D. Faires, Numerical Analysis, PWS-KENT, Boston, 1989.
[30] P.M. Adler, C.J. Jacquin, J.A. Quiblier, Flow in simulated porous media, Int. J. Multiphase Flow 16 (1990) 691–712.
[31] E.S. Kikkinides, V.N. Burganos, Structural and flow properties of binary media generated by fractional Brownian motion models, Phys. Rev. E. 59 (1999) 7185–7194.
[32] E.S. Kikkinides, V.N. Burganos, Permeation properties of three-dimensional self-affine reconstructions of porous materials, Phys. Rev. E. 62 (2000) 6906–6915.
[33] F.A. Coutelieris, Modeling of flow and mass transport in granular porous media, Cent. Eur. J. Phys. 9 (2011) 962–968.